

# A Simulation Study of Experimental GaInP/InGaAs/Ge Triple-Junction Solar Cell

Veljko Nikolić, Nebojša Janković

**Abstract** – In this paper, an experimental GaInP/InGaAs/Ge triple-junction (TJ) solar cell is described and fully simulated using the TCAD tool ATLAS/Silvaco. The major stages of the simulation process are explained and the simulation results are compared with experimental data. The simulated and measured results agree well with respect to I-V cell characteristics under the one sun irradiation. Also, low quantum efficiency is obtained from full cell simulation, but requires further cell design optimization.

## I. INTRODUCTION

Multijunction solar cells made of III-V compound semiconductors are the most efficient devices for converting solar radiation into electrical energy. Today, these solar cells are widely used for powering satellites in space, and are started to be used for terrestrial applications through the use of photovoltaic concentrator systems.

Efficiencies have been dramatically improved in recent years. In 2010, Spire Semiconductor LLC produced a world record efficiency concentrator photovoltaic solar cell. The triple-junction solar cell achieved 42.3% conversion efficiency under a solar concentration of 406 suns [1].

Single solar cells can absorb only a small portion of the solar spectrum. To achieve a higher power density, solar cells with different I-V curves and bandgaps are stacked in order. The top cell has the highest bandgap, while the bottom cell has the lowest. This way, a cell absorbs the photons with energy higher than the bandgap and produces electric power. At the same time, it allows the lower-energy photons to pass through it. This method is called spectrum separation. Unfortunately, stacking the cells this way creates parasitic junctions between dissimilar regions of different cells reducing the current flow. To solve this problem tunnel junctions are used for separating individual cells. Tunnel junctions allow the photons to pass through as well as current with minimal voltage loss [2].

In this work, an experimental GaInP/InGaAs/Ge triple-junction (TJ) solar cell is described and fully simulated using the Technology Computer Aided Design (TCAD) tool ATLAS/Silvaco. In order to provide an accurate simulation, specific parameters needed to be inserted into the material related models. The exotic

materials used in this device were carefully studied and all their major electrical and optical parameters were researched or derived. Three individual cells were first developed and tested individually. This way, their efficiency was optimized and their performance characteristics were adjusted to the required range. Material and model parameters were optimized to reach a better approximation. This process was repeated several times until the results were accurate enough. Short circuit currents and open circuit voltages were obtained. J-V curves and frequency responses are also plotted. An identical process was done with the tunnel junctions. Finally, the complete triple-junction structure was simulated.

## II. TJ CELL STRUCTURE

The Simulated structure of fabricated experimental TJ collar cell [3] is schematically shown in Fig. 1.

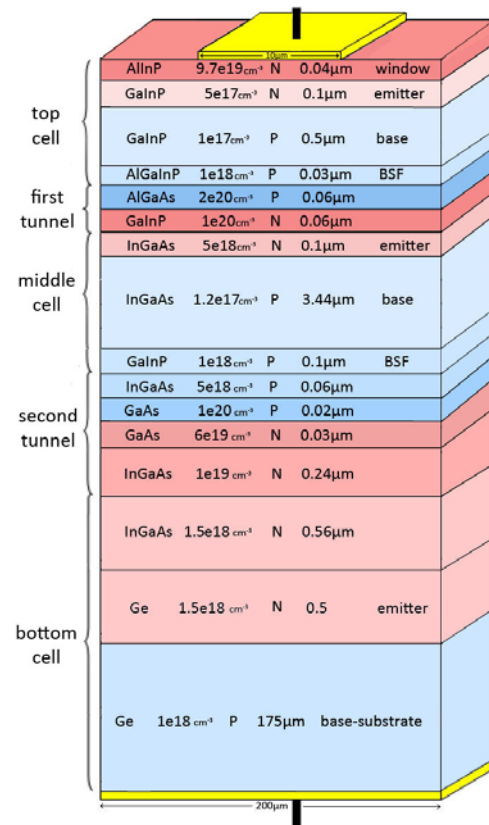


Fig. 1. Triple junction solar cell

Nebojša Janković is with the Department of Microelectronics, Faculty of Electronic Engineering, University of Niš, Aleksandra Medvedeva 14, 18000 Niš, Serbia,  
E-mail: nebojsa.jankovic@elfak.ni.ac.rs

In the cell, the Ge substrate acts as a base for the bottom cell. On top of it are the Ge emitter and two layers of InGaAs which form a heterostructure. Next is the second tunnel junction consisting of two heavily doped n- and p-type GaAs layers. A thin InGaAs window layer comes after, followed by a GaInP BSF layer. InGaAs middle cell is stacked next, on top of the cell is the first tunnel junction formed by heavily doped layers of n-type GaInP and p-type AlGaAs. Then come AlGaInP BSF layer, the top cell from GaInP and an AlInP window. All contacts are made of gold.

A window layer is used in order to reduce the surface recombination velocity. Similarly, a BSF layer reduces the scattering of carriers towards the tunnel junction. Both layers have a heterojunction structure and are used for lattice matching. Also, they must be transparent to wavelengths absorbed by the next cell.

### III. DEVICE SIMULATION

Silvaco TCAD software package is a large suite of highly sophisticated tools for design and development of all types of semiconductor devices. It contains ATLAS, a physically based device simulator which calculates electrical characteristics of the device's physical design and bias conditions [4].

The modules required for Solar Cell simulation include: S-Pisces, Blaze, Luminous, Device3D, Luminous3D. S-Pisces is an advanced 2D device simulator for silicon based technologies that incorporates both drift-diffusion and energy balance transport equations. Blaze simulates 2D solar cell devices fabricated using advanced materials. It includes a library of binary, ternary and quaternary semiconductors. Device3D simulates DC, AC and time domain characteristics for silicon and other material based technologies. Luminous and Luminous3D are advanced simulators specially designed to model light absorption and photogeneration in non-planar solar cell devices. Exact solutions for general optical sources are obtained using geometric ray tracing. This feature enables Luminous and Luminous3D to account for arbitrary topologies, internal and external reflections and refractions, polarization dependencies and dispersion. It also allows optical transfer matrix method analysis for coherence effects in layered devices. The beam propagation method may be used to simulate coherence effects and diffraction. [4]

When interference effects are important, such as in the presence of an antireflective coating or when the semiconductor absorption layers are thin, using traditional ray-tracing is useless because reflected rays in each layer need to be set to a very large number and that would exponentially increase the time of the simulation. The only way to achieve a good accuracy is to use the transfer matrix method. This approach relates total tangential components of the electric and magnetic fields at the multilayer boundaries. The structure of a multilayer completely

determines the characteristic matrix of this multilayer. The transfer matrix also contains information about the media on both sides of the multilayer. [5]

There are five groups of physical models in ATLAS: mobility, recombination, carrier statistics, impact ionization, and tunnelling. They can be specified for each material. In Atlas simulations, we have included the Shockley-Read-Hall generation/recombination model, bandgap narrowing, Fermi-Dirac carrier statistics, and the non-local band to band tunnelling model.

Across highly doped junctions, the band-to-band tunnelling current can be very high and it depends very strongly on the band edge profile throughout the junction. In turn, the injected tunnel current creates a charge dipole and strongly affects the potential, and consequently the band energies, at and near the junction. This strong coupling can cause convergence problems in some situations. Non-local coupling and band-to-band forward models are used to mitigate these problems. Band to band optical generation/recombination (radiative) model is important for narrow gap semiconductors and semiconductors whose specific band structure allows direct transitions. [4]

The mesh is very important for the final accuracy of the simulation. The density needs to be high near regions such as junctions, material boundaries, or electrodes. If not, the results could be inaccurate and misleading. On the other hand, creating a thicker mesh increases simulation time. One part of the mesh structure is shown in Fig. 2.

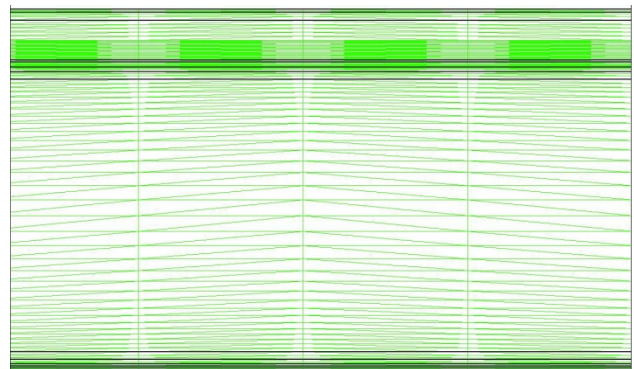


Fig. 2. Insight into the 2D Meshing of TJ solar cell

The tunnelling layer can be modelled as being one-dimensional in nature so that it can be calculated using a special rectangular mesh superimposed over and coupled to the ATLAS mesh. This mesh needs to include the junction region of interest and the direction of band-to-band tunnelling, which is generally perpendicular to junction interface.

Because of their electro-optical nature, the simulation of solar cells must necessarily take into account many detailed phenomena. From the optics point of view, the

simulator must allow the definition of standard solar spectra, such as AM1.5 (Fig. 3).

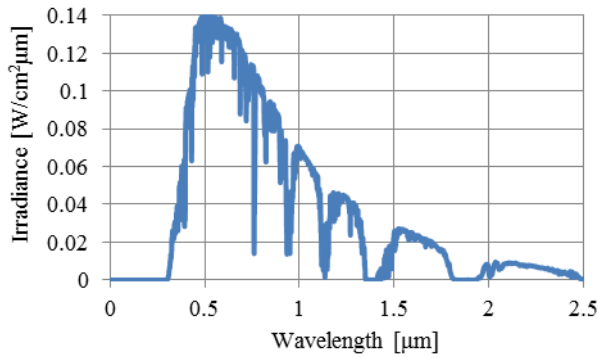


Fig. 3. Air mass spectrum 1.5

All simulations were performed at room temperature (27°C) and AM1.5 with one sun intensity.

#### A. Individual Cell Simulation

Current-voltage characteristics of the three individual solar cells are shown in Fig. 4. GaInP cell has an open circuit voltage ( $V_{OC}$ ) of 1.405V, InGaAs has 0.945V and Ge has 0.347V. GaInP cell has the largest bandgap and should produce less current then the others, but in this case the additional layers contribute so the top cell has the highest current density. Fig. 4 shows that the InGaAs middle cell limits the short-circuit current in TJ cell and should be further optimized.

Quantum efficiencies of the solar cells under a concentration of one sun are displayed in Fig. 5. As previously mentioned, GaInP cell has the largest bandgap. Therefore, the top cell absorbs higher energy photons and lets the lower energy photons pass through. The lower energy photons continue to the middle cell, one number of photons is absorbed here and the rest pass through to the bottom cell. Ge has a low attenuation coefficient, so Ge layers are always built thick.

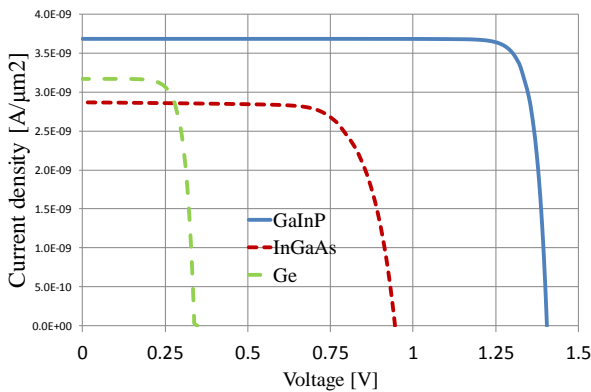


Fig. 4. J-V characteristics of single solar cells

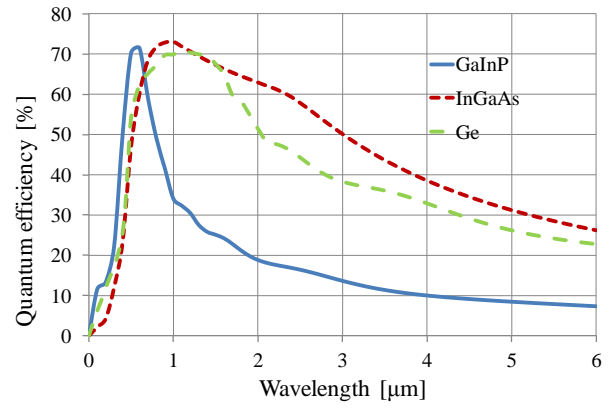


Fig. 4. Spectrum separation

The examples of real and imaginary optical indexes  $n$  and  $k$  of the cell's main materials, for wavelengths in the range from 0.2μm to 1.2μm, are shown in Figs. 6 and 7, respectively. These values and the indexes for other semiconductors in the TJ cell structure were inputted into ATLAS externally as separate material files. The data were collected from available literature. However, only a small number of data is published for ternary and quaternary materials, therefore some values had to be interpolated at higher wavelengths.

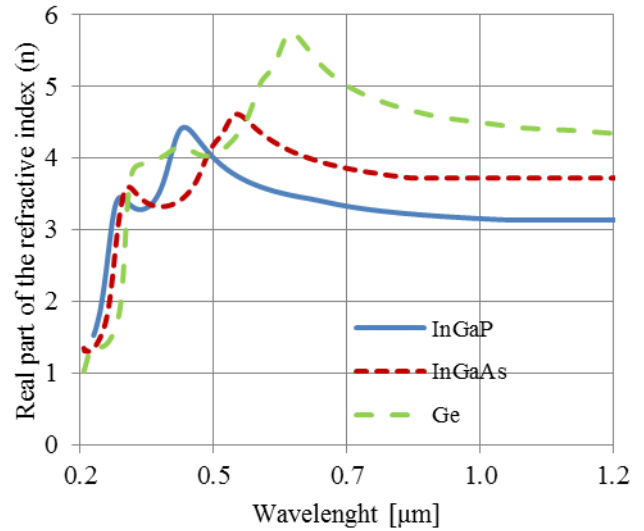


Fig. 6. Real part of the refractive index vs. wavelength

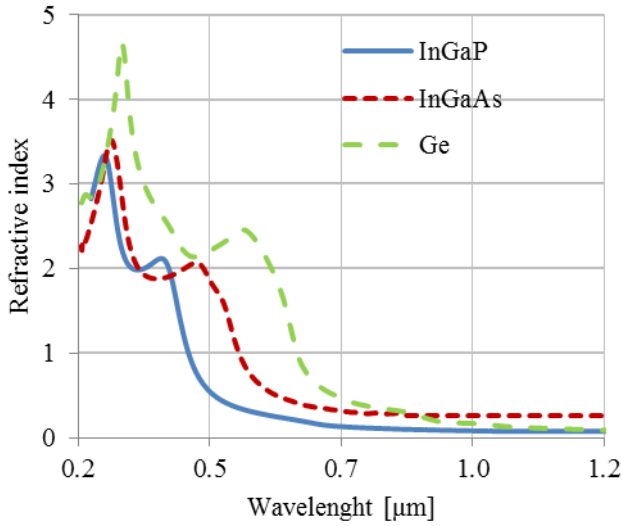


Fig. 7. Extinction coefficient vs. wavelength

### B. Tunnel Junction Simulation

Tunnel junction is a very important layer, essential in the vertical stacking of more than one cell, in order to construct a multi-junction configuration. It should be optically transparent and connect the component cells in the multijunction structure with the minimum of electrical resistance. The optical absorption in the tunnel junction is minimised by using thin layers of wide bandgap materials, although care must be exercised as the tunnelling current decreases exponentially with increasing band-gap energy [4].

Fig. 8 shows J-V characteristics of both tunnel junctions, simulated without irradiance. It is found that the GaAs tunnel diode exhibits a smaller dynamic resistance in comparisons with the AlGaAs/GaInP tunnel diode.

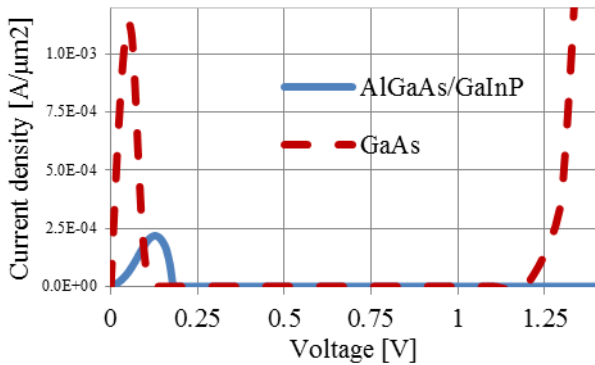


Fig. 8. Tunnel junction J-V characteristics

### C. Complete Cell Simulation

Simulated J-V characteristic of the complete triple-junction solar cell is shown in Fig. 9. The predicted open

voltage of the TJ cell has a  $V_{OC}=2.47V$ , while the cumulative open circuit voltage of individual cells is 2.697V, obtained from Fig.4. This difference can be attributed to the voltage drop on the two tunnel junctions. The experimental data, obtained from IQE Europe Ltd. Manufacturing [3], are also displayed in Fig. 9.

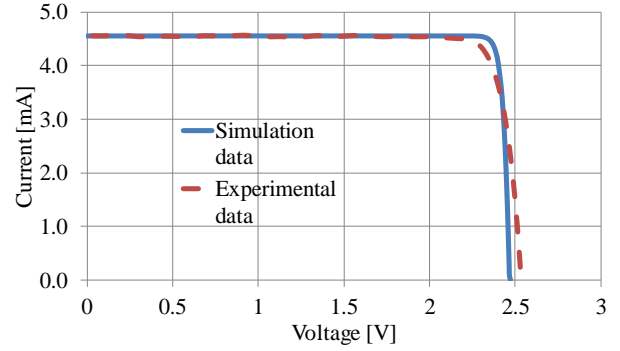


Fig. 9. J-V characteristic of the triple-junction solar cell

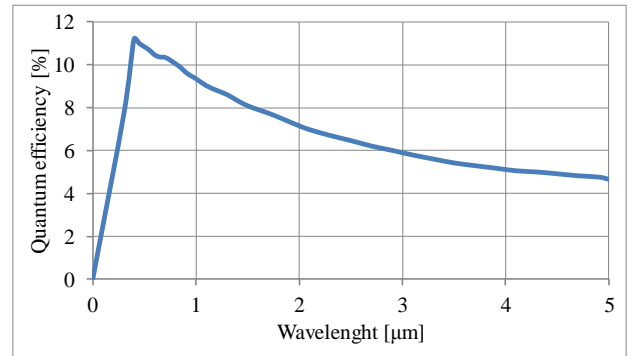


Fig. 10. Quantum efficiency of the triple-junction solar cell

The simulated external quantum efficiency of the complete TJ solar cell is shown in Fig. 10. The obtained cell efficiency is not satisfying, but at the time or writing this paper, the experimental data were not available and the simulation results need to be verified.

Fig. 11 displays the total current density flow of the top cell and the first tunnel junction. As shown in the figure, the maximum current density is located near the top contact, the cathode. Inside the tunnel junction, the current is not defined because the Ohm's law doesn't apply here, only quantum tunnelling.

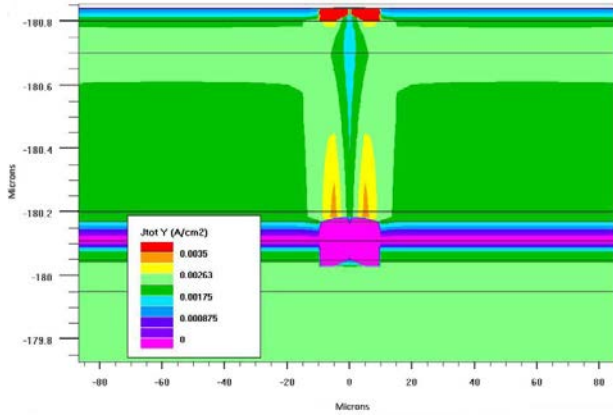


Fig. 11. Total current density flow

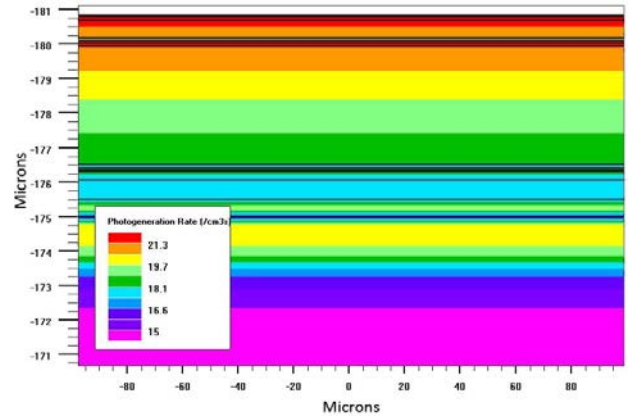


Fig. 13. Photogeneration rate

Photogeneration rate graphs are shown in Figs. 12 and 13. Individual solar cells produce current in different wavelengths, according to their frequency response. The highest photogeneration rate is in the upper layers because they are exposed to a greater number of photons. If the solar cells are observed individually, all emitters have a higher photogeneration rate than their bases.

Band energy diagram of the TJ solar cell with several heterojunctions is shown in Fig. 14.

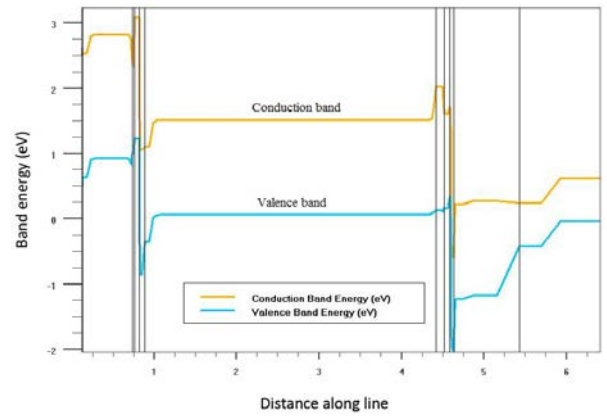


Fig. 14. Band energy diagram

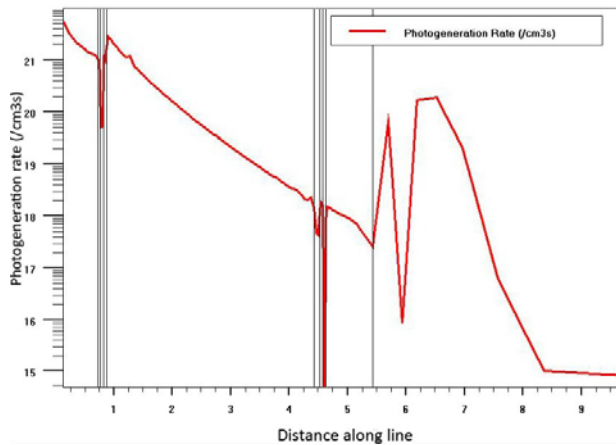


Fig. 12. Photogeneration rate through cross section

Finally, all materials used for building the triple-junction solar cell, with their parameters used in ATLAS simulation package are given in Table 1. The table illustrates all the complexity of the TJ cell simulation and the immense task for simulator calibration due to involving many physical, optical and material parameters that need to be carefully selected and verified.



## ACKNOWLEDGEMENT

The authors would like to thank IQE Europe Ltd. Manufacturing for providing us with experimental data on TJ solar cell.

## REFERENCES

- [1] "Spire pushes solar cell record to 42.3%", 7.10.2010. <http://optics.org/news/1/5/5>
- [2] T. Michalopoulos, "A novel approach for the development and optimization of state-of-the-art photovoltaic devices using Silvaco", 2002.
- [3] "IQE Europe Ltd. Manufacturing". <http://www.iqep.com>
- [4] "Silvaco ATLAS User's Manual", 2010. <http://www.silvaco.com>
- [5] M. Baudrit, C. Algara, "Modeling of GaInP/GaAs Dual-Junction Solar Cells including Tunnel Junction", 2008.

Table 1  
Material properties

Parameter	Material						
	GaAs	GaInP	Ge	AlGaAs	AlInP	AlInGaP	InGaAs
$E_g$ [eV]	1.424	1.9	0.661	1.8	2.4	2.4	1.45
$\epsilon$	12.9	11.62	16.2	12.3	11.7	11.7	11.7
$q\chi_s$ [eV]	4.07	4.08	4	3.54	4.2	4.2	4.05
$N_A$ [cm <sup>-3</sup> ]	4.7e17	1.3e20	1e19	4.35e17	1.08e20	1.2e20	3.2e19
$N_D$ [cm <sup>-3</sup> ]	9e18	1.28e19	5e18	8.16e18	1.28e19	1.28e19	1.8e19
$C^{eff}$ [cm <sup>-2</sup> s <sup>-1</sup> ]	7.2e-10	1e-10	6.41e-14	1.5e-10	1.2e-10	1e-10	7.2e-12
$\mu_n$ [cm <sup>2</sup> /Vs]	8000	4000	900	2000	2291	2150	300
$\mu_p$ [cm <sup>2</sup> /Vs]	400	1000	900	100	142	141	1
AUGN [cm <sup>2</sup> s <sup>-1</sup> ]	5e-30	3e-30	1e-30	5e-30	9e-31	3e-30	/
AUGN [cm <sup>2</sup> s <sup>-1</sup> ]	1e-31	3e-30	1e-30	1e-31	9e-31	3e-30	/
$m_n$ $m_0$	0.001	0.1	0.2	0.1	0.2	0.2	0.2
$m_p$ $m_0$	0.01	0.1	0.2	0.1	0.2	0.2	0.2

## IV. CONCLUSION

In summary, a separated single junction GaInP, InGaAs and Ge solar cells were successfully simulated along with AlGaAs/GaInP and GaAs/GaAs tunnel junctions. Material and model parameters were optimized to achieve a better match with the experimental data. The single junction cells were then combined into a stacked triple-junction solar cell which was also successfully simulated as a whole. Basic physical quantities such as band diagrams, optical photogeneration rate and current density are demonstrated. The simulated J-V characteristics of analysed TJ solar cell shows a close match with the experimental results obtained from the fabricated test TJ solar cell.

To the best of our knowledge, no published papers in conferences or journals reported a full simulation of a complete TJ multijunction solar cell, especially not the ones with simulations of its quantum efficiency. This conference paper is the first to show that the TJ solar cell with two tunnel junctions can be successfully simulated using Silvaco TCAD tools.